

## Energy bands of (100) and (110) ferromagnetic Ni films

D. G. Dempsey, W. R. Grise, and Leonard Kleinman

Department of Physics, University of Texas, Austin, Texas 78712

(Received 15 February 1978)

We discuss the procedure for obtaining the linear-combination-of-atomic-orbitals Hamiltonian and overlap parameters to fit the bulk energy bands of Ni. We then describe an internally consistent method for obtaining the shifts of the surface intra-atomic  $d$  parameters. The energy bands and planar densities of states of a 35-layer (100) and 47-layer (110) Ni film are calculated. Surface states exist above the majority-spin  $d$  bands throughout the two-dimensional Brillouin zone in the (100) case. Transitions from these surface states into an evanescent low-energy-electron-diffraction state account for the reversal of photoelectron spin polarization observed 0.1 eV above threshold in the (100) case.

### I. INTRODUCTION

Transition-metal-surface or thin-film energy-band calculations are still in a very primitive stage. The only self-consistent  $3d$ -transition-metal surface calculation in the literature<sup>1</sup> was performed for Cu which is much easier to handle than metals with partially filled  $3d$  bands. The calculation was done for a film of only three layers which made it impossible to distinguish surface states from bulk states. Finally this linear combination of atomic orbitals (LCAO) calculation used an incomplete basis set; the  $4p$  orbital (which is the major orbital for those states in the neck of the Fermi surface) was not included in the expansion. A few *ab initio* calculations<sup>2,3</sup> have been performed for thicker films. Unlike bulk-band calculations, where a superposition of atomic charge densities yields a crystal potential not too far from the self-consistent potential, there is a large charge redistribution near the surface and although many interesting surface effects can be seen, the results are not quantitatively accurate. There have been several parametrized transition-metal-film calculations.<sup>4-6</sup> The parameters for the interior atoms can be obtained with an accuracy equal to or better than the accuracy of self-consistent bulk calculations. There are, however, a large number of parameters associated with surface atoms and very little experimental data to guide one in fixing their values. In Sec. II we describe how we obtained our Ni bulk and (100) surface parameters and how with only a single multiplicative parameter we were able to obtain (110) surface parameters from the (100) parameters. Although these techniques are still somewhat crude, we believe that as more experimental data become available, their accuracy will begin to rival that of parametrized bulk-energy-band calculations.

In Sec. III the planar densities of states (PDOS) and two-dimensional (2D) energy bands of 35-layer

(100) and 47-layer (110) Ni films are displayed and some important surface states are discussed. In Sec. IV we calculate the polarization of photoelectrons emitted from a (100) Ni surface. Our band calculation yields a photoelectron spin polarization which is negative at threshold but which changes sign only 0.12 eV above threshold, in excellent agreement with the data of Eib and Alvarado.<sup>7</sup>

### II. BULK AND SURFACE PARAMETERS

The primary criterion the surface parameters must satisfy is that of surface-charge neutrality. Self-consistent calculations in nearly-free-electron metals indicate that a single plane should be neutral to within 0.03 or 0.04 electrons per atom and the net charge on the first two or three planes should be an order of magnitude smaller.<sup>8</sup> Since surface-charge discrepancies as large as 0.9  $d$  electrons per atom and 0.5  $sp$  electrons per atom have been found<sup>9</sup> when bulk parameters are used at the surface, this is a powerful criterion. We have recently shown<sup>10</sup> that if one does not make the assumption of orthogonality between orbitals on different sites, there is a continuum of sets of parameters which fit the bulk-energy bands equally well, corresponding to a continuum of sets of basis functions. At one extreme Wannier functions can be used and at the other extreme atomiclike orbitals can be used. Because a Wannier function is orthogonal to the neighboring Wannier functions, the neighboring sites appear repulsive to a Wannier function; on the other hand, the attractive potential makes the neighboring sites appear attractive to atomic orbitals. Therefore there exists a set of orbitals intermediate to Wannier and atomic orbitals for which neighboring sites will appear neutral. For this set of basis functions the surface may be only a minor perturbation on the diagonal matrix elements. There are charge redistribution effects on the potential at the surface but for the  $s$

and  $p$  electrons which are not localized and therefore sample the entire surface these seem to affect the diagonal matrix elements in about the same way for all crystal surfaces. Thus this effect may be compensated for by a choice of orbitals for which the neighboring sites are not quite neutral. Of course one never finds the orbitals; one finds their Hamiltonian and overlap matrix element parameters. In copper where the  $d$  bands are filled, we were able to find a set of bulk parameters which gave surface charge neutrality with no surface parameter shifts for not only the (100), (110), and (111) surfaces<sup>10</sup> but for a stepped surface as well.<sup>11</sup>

Since without a completely self-consistent calculation one cannot know how much charge is transferred between the  $sp$  and  $d$  bands at the surface, we base our Ni parameters on Cu as much as possible. We first made a semirigid shift of the Cu bands by setting

$$H_{p'l'l'm}^{\sigma} = H_{p'l'l'm}^{\text{Cu}} + \frac{1}{2}(\Delta E_l^{\sigma} + \Delta E_{l'}^{\sigma})S_{p'l'l'm}^{\text{Cu}}, \quad (1)$$

where  $E_s^{\sigma}$ ,  $E_p^{\sigma}$ , and  $E_d^{\sigma}$  are three parameters chosen to fit Wang and Callaway's<sup>12</sup> (WC) energy bands of spin polarization  $\sigma$  (calculated with the von Barth and Hedin exchange and correlation potential) as well as possible. (Note that to shift the bands rigidly by an amount  $\Delta E$ , one must change the Hamiltonian parameters by an amount  $\Delta H_{p'l'l'm} = \Delta E S_{p'l'l'm}$ , where  $S_{p'l'l'm}$  is the overlap between  $l$  and  $l' = s, p$ ,

or  $d$  basis functions with azimuthal quantum number  $m$  which are  $p$  neighbors apart.) With the  $H_{p'l'l'm}^{\sigma}$  and  $S_{p'l'l'm}^{\text{Cu}}$  as starting values, we ran our rms error minimization routine to fit the bulk Ni bands at 43 points in the  $\frac{1}{48}$  irreducible Brillouin zone (BZ) with rms errors of only  $2.56 \times 10^{-3}$  and  $2.45 \times 10^{-3}$  Ry in the majority- and minority-spin bands. The largest error in any energy level was  $8.89 \times 10^{-3}$  Ry. Because the zero of energy in bulk-energy bands is completely arbitrary, we shifted the WC bands rigidly upwards by 0.1542 Ry before making the fit; this will allow us to obtain the correct work function for the (100) film. Because WC's bands have too large an exchange splitting we raised the majority spin intra-atomic  $d$  parameter ( $dd_0$  in Table I) by 0.10 Ry after we had fit their bands. This yields a splitting of 0.50 eV for the  $X_5$  bulk state in agreement with experiment<sup>12</sup> and a magneton number (0.54) in good agreement with the experimental value of<sup>12</sup> 0.56. This final set of parameters (ten two-center Hamiltonian and overlap parameters for each of three neighbors and  $s$ ,  $p$ , and  $d$  intra-atomic or zeroth-neighbor Hamiltonian parameters for each spin) is displayed in Table I. The third-neighbor overlap and Hamiltonian parameters are all small and a reasonable fit could have been obtained without them; however, we have in the past, when fitting a smaller sample of points in the BZ, found that our rms fitting routine could

TABLE I. Final set of bulk-energy-band  $n$ th-neighbor Hamiltonian ( $H_n$ ) parameters (in Ry) and overlap ( $S_n$ ) parameters for ferromagnetic nickel.

	Majority $ss_0 = -0.30632$ $pp_0 = 0.19039$ $dd_0 = -0.50094$					
	$H_1$	$H_2$	$H_3$	$S_1$	$S_2$	$S_3$
$ss\sigma$	-0.13274	-0.02719	-0.00141	0.08264	0.00480	0.00056
$pp\sigma$	0.17274	0.09368	0.01471	-0.21102	-0.04091	-0.00165
$pp\pi$	-0.05602	-0.01892	0.00105	0.05336	0.03222	0.01358
$dd\sigma$	-0.03391	-0.00299	0.00001	0	0	0
$dd\pi$	0.01902	0.00048	0.00007	0	0	0
$dd\delta$	-0.00322	0.00008	-0.00000	0	0	0
$sp\sigma$	0.15630	0.03810	0.00716	-0.12792	0.01036	-0.00259
$sd\sigma$	-0.04633	-0.01106	0.00006	0	0	0
$pd\sigma$	-0.04830	-0.01064	-0.00035	-0.01796	0.00301	0
$pd\pi$	0.04132	0.00060	-0.00048	-0.01657	-0.00023	0
	Minority $ss_0 = -0.30188$ $pp_0 = 0.19796$ $dd_0 = -0.47108$					
	$H_1$	$H_2$	$H_3$	$S_1$	$S_2$	$S_3$
$ss\sigma$	-0.13277	-0.02794	-0.00147	0.08187	0.00344	0.00109
$pp\sigma$	0.16600	0.08911	0.00822	-0.19010	-0.04174	-0.00418
$pp\pi$	-0.05728	-0.01644	0.00043	0.03845	0.01076	0.01011
$dd\sigma$	-0.03595	-0.00333	-0.00001	0	0	0
$dd\pi$	0.01983	0.00067	0.00003	0	0	0
$dd\delta$	-0.00296	0.00008	-0.00000	0	0	0
$sp\sigma$	0.16235	0.05600	0.00607	-0.13058	-0.01753	-0.00222
$sd\sigma$	-0.04892	-0.00976	0.00006	0	0	0
$pd\sigma$	-0.04868	-0.01141	-0.00025	-0.02260	0.00012	0
$pd\pi$	0.04357	0.00079	-0.00037	-0.02159	-0.00006	0

converge to an incorrect set of parameters (which failed to fit additional points in the BZ) but these parameters had the unphysical property that several of the third-neighbor parameters were quite large. Therefore we always use third-neighbor parameters, both for the slight improvement they give to the fit and as a check on the physical nature of the parameters. Not counting third neighbors and the vanishing  $dd$  and  $sd$  overlap parameters, there are effectively 35 parameters with which we fit a total of 238 independent energy levels. The vanishing of the  $dd$  and  $sd$  overlap parameters is a consequence of a theorem of Anderson<sup>13</sup> which states that if one can construct the crystal potential out of a superposition of overlapping spherical potentials, and if the overlap between orbitals is small, then to first order in that overlap the secular equation contains no overlap terms and the diagonal matrix elements are just the energy of the orbitals in the potential from their own site. That is, the attractive potential and repulsive overlap of the neighbors cancel to first order. This then also explains why we have never found<sup>4(a), 5(a)</sup> any cubic crystal-field splitting of the  $xy$  and  $x^2 - y^2$   $dd_0$  intra-atomic parameters for  $3d$  transition metals. It is interesting to note that in tungsten,<sup>14</sup> where the  $5d$  functions have a large overlap, we found it impossible to fit the bulk-energy bands with Wannier parameters until we allowed the  $xy$  and  $x^2 - y^2$   $dd_0$  parameters to assume different values.

One might naively think because the neighboring atoms appear neutral to the diagonal  $d$  matrix elements, that  $dd_0$  matrix element shifts at the surface would not be required (as is the case for  $ss_0$  and  $pp_0$ ). However, the missing off-diagonal matrix elements cause the surface PDOS to be much narrower than that for interior planes; thus more of the surface PDOS lies below  $E_F$ , giving a large surface-charge surplus which causes a repulsive potential which does affect the diagonal  $d$  matrix elements. This  $d$ -band surface narrowing has been observed<sup>15</sup> experimentally in Cu to be in excellent agreement with our Cu calculations.<sup>10</sup> In Cu because the  $d$  bands are full, this does not affect the  $dd_0$  matrix elements appreciably which is consistent with the experimental fact that surface Cu core-energy levels are not shifted from bulk values.<sup>15</sup> Using these parameters we calculated the energy bands of a 35 layer (100) Ni film at  $N = 576$  points in the 2D BZ (91 points in the  $\frac{1}{8}$  irreducible 2D BZ). We calculated the local DOS for symmetry  $\alpha$ , spin  $\sigma$ , and plane  $i$ , using the formula

$$n_{i\alpha\sigma}(E) = N^{-1} \sum_{j\beta n\bar{k}} W(\bar{k}) C_{\alpha i}^{n\bar{k}\sigma} S_{ij}^{\alpha\beta}(\sigma, \bar{k}) \quad (2)$$

$$\times C_{\beta j}^{n\bar{k}\sigma} \delta(E - E_{n\bar{k}}),$$

where the  $\bar{k}$  sum is over the 91 points in the  $\frac{1}{8}$  2D BZ and  $W(\bar{k})$  is the number of times each such point occurs in the full 2D BZ,  $C_{\alpha i}^{n\bar{k}\sigma}$  is the coefficient of the  $i$ th planar ( $\alpha, \sigma$ ) Bloch function appearing in the  $n$ th eigenfunction at  $\bar{k}$ , and  $S_{ij}^{\alpha\beta}(\sigma, \bar{k})$  is the overlap of the two planar Bloch functions ( $i, \alpha$ ) and ( $j, \beta$ ). A preliminary calculation with no surface parameter shifts found a surface surplus of 0.1135 majority  $d$ , 0.4507 minority  $d$ , 0.0398  $s$ , and a deficit of 0.1388  $p$  electrons per surface atom. The majority-spin  $d$  bands are filled; there are, however, about 0.3 majority-spin  $d$  electrons per atom hybridized into bands above  $E_F$ . The surface-majority-spin  $d$  electron surplus arises from a decrease in hybridization at the surface. Because of the reduced symmetry at the surface there are four independent surface  $dd_0$  parameters per spin. Because we were convinced that the photoelectron spin-polarization reversal<sup>7</sup> could be understood only if a surface state existed several hundredths of an eV above the majority spin  $d$  bands at the center ( $\bar{\Gamma}$ ) of the 2D BZ, we took that and surface-charge neutrality as our two principle criteria for determining the eight surface-parameter shifts. The surface-parameter shifts together with the charge in each orbital on the surface and central planes are shown in Table II. In order to obtain a  $\bar{\Gamma}_5$  surface state the  $(xz, yz)_\dagger$  shift had to be 0.042 Ry; in order to get the  $\bar{\Gamma}_5$  surface state 0.06 eV above the top of the  $d$  bands we took the shift to be 0.052 Ry. Because the lobes of the  $xz$  and  $yz$  orbitals point directly toward missing neighbors the  $(xz, yz)$  surface shift is the largest and the other majority-spin-surface parameter shifts were es-

TABLE II. Intra-atomic  $d$  parameter (100) surface shifts (in Ry) and charge associated with each orbital in the surface and central planes. ( $xy$  and  $x^2 - y^2$  are referred to the square 2D lattice which is rotated  $45^\circ$  with respect to the cubic lattice.)

	Shift	$\rho$ (surf)	$\rho$ (cent)
$(xy)_\dagger$	0.030	0.9417	0.9461
$(xy)_\ddagger$	0.020	0.8731	0.8784
$(xz, yz)_\dagger$	0.052	0.9545	0.9265
$(xz, yz)_\ddagger$	0.038	0.7879	0.7803
$(x^2 - y^2)_\dagger$	0.022	0.9108	0.9261
$(x^2 - y^2)_\ddagger$	0.013	0.8049	0.7811
$(3z^2 - r^2)_\dagger$	0.035	0.9496	0.9454
$(3z^2 - r^2)_\ddagger$	0.024	0.9085	0.8791
Total $\rho_d$		8.873	8.770
$(s)_\dagger$		0.3363	0.3113
$(s)_\ddagger$		0.3386	0.3178
$(x, y)_\dagger$		0.0843	0.0963
$(x, y)_\ddagger$		0.0926	0.1043
$(z)_\dagger$		0.0487	0.0964
$(z)_\ddagger$		0.0528	0.1043
Total $\rho$		10.004	10.001

timated according to how their lobes point relative to the missing atoms outside the crystal. The minority-spin parameter shifts were chosen to be sufficiently smaller than the corresponding majority-spin shifts so that surface-charge neutrality was obtained. We note that even with the inclusion of the repulsive surface-parameter shifts ( $xz, yz$ ) which sees the largest shift and  $3z^2 - r^2$  which sees the second largest have the largest and second largest surface charge excesses, respectively (as compared to the central plane charge). This is a strong indication that their shifts are not too large relative to the surface shifts of the other two  $d$  orbitals. On the other hand, the minority-spin shifts seem somewhat too small relative to the majority-spin shifts. We note from Table II that the  $s$  and transverse  $p$  orbitals together are equally occupied on the surface and central planes but the longitudinal  $p$  orbitals suffer a surface-charge deficit of 0.10 electron. This seems entirely reasonable to us and is a consequence of our basing our bulk Ni parameters upon the Cu parameters. We could have obtained an equally good fit to the bulk Ni bands using  $s$  and  $p$  parameters which would have led to  $sp$  surface charge neutrality. Then because we would no longer need a  $d$  surface surplus to compensate the  $p$  deficit, our minority  $d$  surface parameter shifts would be larger. Which of these pictures is more nearly correct cannot be determined until more surface data becomes available to fit.

After completing this calculation we realized that we could reduce the number of independent  $d$  surface-shift parameters by making the same two-center<sup>16</sup> approximation that we make in the bulk Hamiltonian except that the wave functions are on one atom and the potential is restricted to the missing nearest-neighbor atoms. The two-center parameters listed in Table III, when multiplied by the appropriate direction cosines<sup>16</sup> and summed over the four missing nearest neighbors outside the (100) surface, yield the surface parameter shifts of Table II to within 5%. Were we to repeat this calculation with no additional experimental data to fit, we would reduce the number of independent surface parameters from eight to four by taking three two-center parameters for one spin and a single multiplicative factor times them for the other spin as our independent parameters.

The surface shifts in matrix elements for the (110) film were calculated from the two-center parameters of Table III multiplied by a single additional parameter (whose value is 0.886), chosen to yield (110) surface charge neutrality. Note in Table IV, that this yields an off-diagonal intra-atomic matrix element which we would be hard pressed to estimate in any other manner; it also yields di-

TABLE III. Two-center surface shift parameters chosen to fit the parameters of Table II.

	Majority	Minority
$dd\sigma^*$	$2.722 \times 10^{-2}$	$2.131 \times 10^{-2}$
$dd\pi^*$	$9.436 \times 10^{-3}$	$6.544 \times 10^{-3}$
$dd\delta^*$	$8.284 \times 10^{-4}$	$-5.735 \times 10^{-4}$

agonal intra-atomic matrix element shifts in the first interior plane. We have previously found<sup>4(c)</sup> for (111) iron (this is the open face in bcc crystals), where the first interior-plane atoms are also missing a nearest neighbor, that we could not get charge neutrality in both the surface and first interior planes without having parameter shifts in both planes. We note from the last three columns of Table IV, that these parameters yield charge neutrality in the surface and first-interior planes. We also note that although the charge associated with individual  $d$  orbitals differs considerably between the first interior and central planes, their total  $d$  charge is identical, whereas the surface plane has a  $d$  surplus of 0.16 electrons per atom which cancels an  $sp$  deficit.

We have not taken account of surface relaxation in this calculation. LEED studies<sup>17</sup> show that the (100) surface expands between 0% and 2.5% and the (110) surface contracts by -5%. However, different LEED beams show<sup>18</sup> the (110) relaxation between +2% and -8% so that the -5% estimate may not be very accurate. The effect of relaxation on the intra-atomic matrix elements may be assumed to be included within the multiplicative parameter chosen to yield charge neutrality because as long as the relaxation is simple (no reconstruction), the symmetry is unchanged. We have not included surface shifts of interatomic matrix elements anywhere in our parametrization scheme (except, of course, that matrix elements connecting an atom to atoms outside the surface vanish). Relaxation changes the surface bond angles which can easily be taken account of in the calculation; it also changes the magnitude of the surface interatomic parameters. The latter cannot be estimated with much accuracy because the basis functions are not simple exponentials. One might, however, expect that because of the freedom one has in choosing the basis functions, most of the interatomic surface shift that would be needed if Wannier or atomic basis functions were used, can be absorbed into the intra-atomic shifts.

Thus we have developed a procedure for reducing the huge number of independent  $3d$  surface parameter shifts at  $n$  different surfaces of a cubic ferromagnetic metal to  $n+3$  ( $n+2$  for paramagnets). Charge neutrality fixes  $n$  of the parameters and the

TABLE IV. Intra-atomic  $d$  matrix element shifts (in Ry) for the (110) surface plane (S) and first interior plane (S-1), and the charge associated with each  $d$  orbital in the S, S-1, and central (C) planes. The orbitals are referred to the 2D rectangular lattice with  $\hat{z} = (2^{-1/2}, 2^{-1/2}, 0)$ ,  $\hat{x} = (-2^{-1/2}, 2^{-1/2}, 0)$ , and  $\hat{y} = (0, 0, 1)$ .

	Shift(S)	Shift(S-1)	$\rho$ (S)	$\rho$ (S-1)	$\rho$ (C)
$(xy/xy)\dagger$	0.0468	0.0007	0.9366	0.9304	0.9269
$(xy/xy)\ddagger$	0.0331	-0.0005	0.7684	0.7722	0.7805
$(xz/xz)\dagger$	0.0368	0.0084	0.9701	0.9429	0.9459
$(xz/xz)\ddagger$	0.0248	0.0058	0.9310	0.8663	0.8780
$(yz/yz)\dagger$	0.0545	0.0084	0.9356	0.9189	0.9266
$(yz/yz)\ddagger$	0.0395	0.0058	0.8418	0.7736	0.7806
$(x^2 - y^2/x^2 - y^2)\dagger$	0.0293	0.0007	0.9379	0.9289	0.9410
$(x^2 - y^2/x^2 - y^2)\ddagger$	0.0186	-0.0005	0.8556	0.8512	0.8539
$(3z^2 - r^2/3z^2 - r^2)\dagger$	0.0461	0.0243	0.9397	0.9486	0.9328
$(3z^2 - r^2/3z^2 - r^2)\ddagger$	0.0325	0.0189	0.8143	0.8409	0.8054
$(x^2 - y^2/3z^2 - r^2)\dagger$	0.0059	0			
$(x^2 - y^2/3z^2 - r^2)\ddagger$	0.0039	0			
Total $\rho_d$			8.931	8.774	8.772
Total $\rho$			9.988	10.012	10.003

remaining three must be fixed from a knowledge of surface-state locations. In the present calculation only one surface state was fit and the remaining two parameters were estimated so shifts for basis functions whose lobes point away from missing neighbors would be smaller than those for functions whose lobes point toward missing neighbors. This is equivalent to requiring (see Table III)  $dd\sigma^* > dd\pi^* \gg dd\delta^*$ . It should be remembered that these shifts are not directly due to the potentials of the missing neighbors but rather to the charge redistribution caused by the missing neighbors. In addition to the  $d$  surface parameters, the  $ss_0$  and  $pp_0$  bulk parameters must in general be deduced from surface considerations. These parameters depend on our choice of basis functions and equally good fits to the bulk bands can be obtained over a wide range of values; however, the surface results are highly sensitive to the choice. In the present calculation we estimated these parameters from our Cu calculation,<sup>10</sup> thus avoiding the need for a surface fit.

### III. RESULTS

In Fig. 1 we show the PDOS of spin  $\sigma$ ,

$$n_{i\sigma}(E) = \sum_{\alpha} n_{i\alpha\sigma}(E), \quad (3)$$

calculated for the surface, next four interior, and central planes of the 35-layer (100) Ni film at 576 points in the 2D BZ. A Gaussian of 0.003 Ry half-width is centered at each eigenvalue and the contributions of all the Gaussians are summed at every point of the curves (calculated on a mesh of 0.001 Ry). Each Gaussian is normalized to give a unit contribution, making the normalization dependent upon the location of the eigenvalue relative to the

mesh points. This procedure yields much smoother PDOS curves than the procedure we previously used.<sup>4,5</sup> (Compare the surface and central plane PDOS curves here with those in Ref. 19 which differ only in the smoothing procedure.) The same graphs are shown in Fig. 2 for the 47-layer (110) Ni film calculated at 88 points in the  $\frac{1}{4}$  irreducible rectangular 2D BZ (280 points in the full 2D BZ). Because there are more *independent* (110) energy levels sampled<sup>20</sup> than (100) we believe the (110) PDOS curves are slightly more accurate. As usual<sup>4,5,9</sup> the surface PDOS has a smaller second moment than interior PDOS with the effect being more pronounced for the (110) surface than the (100) because of the larger number of missing neighbors. Note that slight differences from the central PDOS exist as far as the fourth plane in from the surface but that the (100) and (110) central PDOS are nearly identical. We may also compare the charge in each orbital in the two central planes. Because of the different coordinate systems used,  $\rho(xy)_{110} \leftrightarrow \rho(yz)_{100}$ ,  $\rho(yz)_{110} \leftrightarrow \rho(zx)_{100}$ ,  $\rho(zx)_{110} \leftrightarrow \rho(xy)_{100}$ ,  $\rho(3z^2 - r^2)_{110} \leftrightarrow \frac{3}{4}\rho(x^2 - y^2)_{100} + \frac{1}{4}\rho(3z^2 - r^2)_{100}$ ,  $\rho(x^2 - y^2)_{110} \leftrightarrow \frac{1}{4}\rho(x^2 - y^2)_{100} + \frac{3}{4}\rho(3z^2 - r^2)_{100}$ . The largest discrepancy is 0.0019 electron/atom between the majority spin  $\rho(3z^2 - r^2)_{110}$  and  $\frac{3}{4}\rho(x^2 - y^2)_{100} + \frac{1}{4}\rho(3z^2 - r^2)_{100}$ . The next largest discrepancy is only 0.0007 electron/atom. This is smaller than the discrepancy between the (100) central plane  $xz$  and  $x^2 - y^2$  minority-spin charges. [Remember  $(x^2 - y^2)_{100}$  is  $xy$  in cubic coordinates.] Whether these small discrepancies are real surface effects extending all the way in to the central plane or are simply noise in the calculation, we cannot say. The Fermi energy, obtained by integrating the total DOS up to 10 electrons/atom, is -0.3804 and

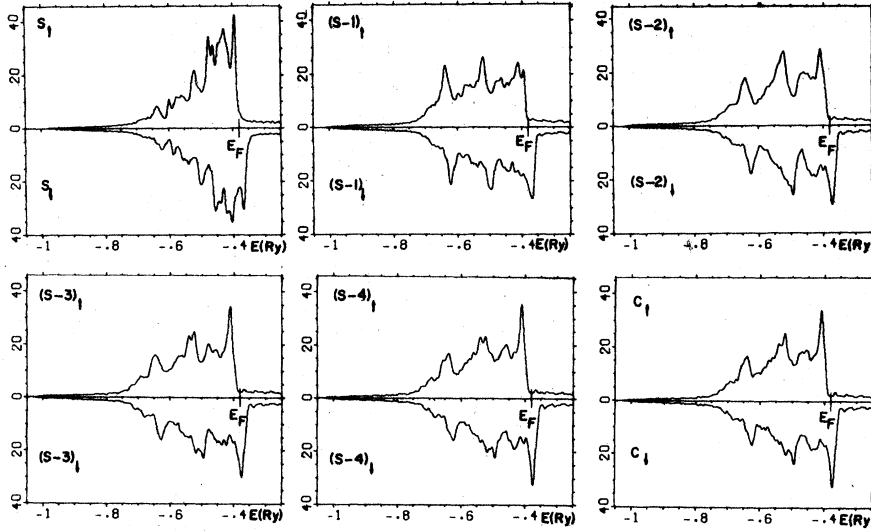


FIG. 1. Majority ( $\uparrow$ ) and minority ( $\downarrow$ ) spin PDOS for the surface (S) and next four interior (S- $n$ ) and central (C) planes of (100) Ni in electrons per atom per Ry.

$-0.3805$  Ry for the (100) and (110) films, the difference being computational noise. This compares well with the (100) work function<sup>7</sup> of 5.15–5.20 eV. If the (110) work function were known, we could easily make a rigid shift of the (110) bands to make them agree.

In Figs. 3 and 4 we display the majority and minority spin-energy bands for the two symmetries along the symmetry lines of the square 2D BZ of the (100) film. We will not discuss the many surface states lying within the various energy gaps except to point out that some of them have been strongly affected by the large surface-parameter shifts and others not. For example, there is a  $\bar{\Delta}_1 - \bar{X}_3 - \bar{Y}_2$  surface state band (with  $\bar{X}_{3\uparrow}$  at  $-0.651$  Ry and  $\bar{X}_{3\downarrow}$  at  $-0.644$  Ry) which is practically identical with a surface-state band<sup>10</sup> in Cu where we

made no surface parameter shifts, except that for Cu the  $\bar{X}$  symmetry is  $\bar{X}_1$ . On the other hand, in the large  $\Sigma_2$  gap around  $-0.5$  Ry we find a  $\Sigma_{2\uparrow}$  surface state band which is somewhat higher relative to the gap than in Cu with the  $\Sigma_{2\uparrow}$  surface state band higher yet. Because the majority-spin-surface-parameter shifts are larger than the minority, we find in addition, a new surface-state band existing only at the bottom center of the  $\Sigma_{2\uparrow}$  gap.

Our main interest is in the surface state pushed out of the top of the  $d$  bands by the surface-parameter shifts. In the majority bands the top of the  $\bar{\Gamma}_5$  bulk continuum is at  $-0.3945$  Ry and the  $\bar{\Gamma}_4$  at  $-0.4069$  Ry. There is a  $\bar{\Gamma}_4$  surface state at  $-0.3978$  Ry and a twofold degenerate  $\bar{\Gamma}_5$  at  $-0.3902$ . Even though the  $\bar{\Gamma}_4$   $xy$  basis function<sup>21</sup> sees a much smaller surface-parameter shift than the  $\bar{\Gamma}_5(xz, yz)$ , the

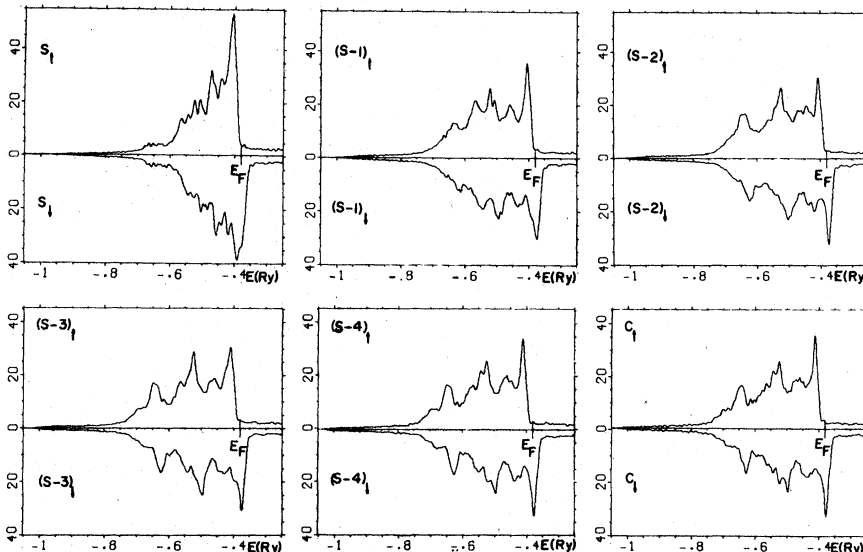


FIG. 2. Majority ( $\uparrow$ ) and minority ( $\downarrow$ ) spin PDOS for the surface (S) and next four interior (S- $n$ ) and central (C) planes of (110) Ni in electrons per atom per Ry.

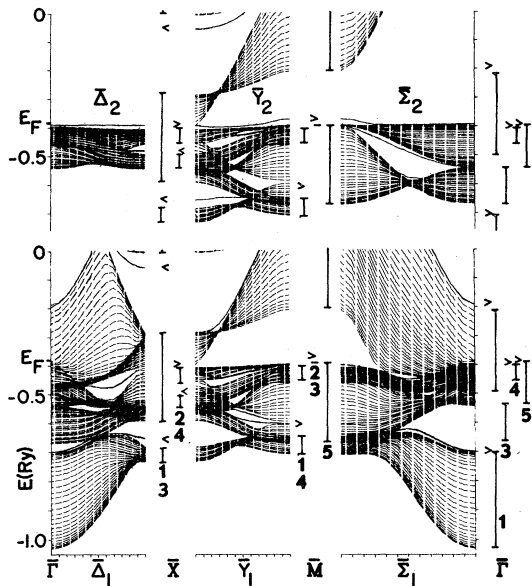


FIG. 3. Majority-spin subbands of  $\bar{\Delta}_1$ - $\bar{Y}_1$ - $\bar{\Sigma}_1$  and  $\bar{\Delta}_2$ - $\bar{Y}_2$ - $\bar{\Sigma}_2$  symmetry for 35-layer (100) Ni film. Solid lines represent surface-state bands. At symmetry points surface states are represented by arrowheads. When two symmetries span the same energy range, a left-pointing arrowhead represents a surface state of higher index symmetry, e.g.,  $\langle$  represents  $\bar{X}_4$ , whereas  $\rangle$  represents  $\bar{X}_2$ .

$\bar{\Gamma}_4$  surface state is pushed more than twice as far out of its continuum. This is because the  $\bar{\Gamma}_5$  continuum is more than twice as wide as the  $\bar{\Gamma}_4$  and because there is a small  $p(x, y)$  admixture in  $\bar{\Gamma}_5$ , whereas  $\bar{\Gamma}_4$  is pure  $d$ .  $\bar{\Gamma}_5$  is compatible with  $\bar{\Sigma}_2$ ,  $\bar{\Delta}_2$  and with  $\bar{\Sigma}_1$ ,  $\bar{\Delta}_1$ , whereas  $\bar{\Gamma}_4$  is compatible with  $\bar{\Sigma}_1$ ,  $\bar{\Delta}_2$ . Thus there exists a  $\bar{\Gamma}_5$ - $\bar{\Sigma}_2$ - $\bar{M}_2$ - $\bar{Y}_2$ - $\bar{X}_2$ - $\bar{\Delta}_2$  surface-state band above the top of the  $d$  bands which becomes a strong resonance at points of no symmetry. In addition there are  $\bar{\Sigma}_1$ - $\bar{\Gamma}_5$ - $\bar{\Delta}_1$  and  $\bar{\Sigma}_1$ - $\bar{\Gamma}_4$ - $\bar{\Delta}_2$  surface-resonance bands which become surface states only at the  $\bar{\Gamma}$  point. These resonances are as sharp as the  $\bar{\Gamma}_5$  and  $\bar{\Gamma}_4$  surface states and extend about  $\frac{1}{3}$  of the way along  $\bar{\Sigma}$  and  $\bar{\Delta}$  to  $\bar{M}$  and  $\bar{X}$ . The  $\bar{\Gamma}_5$  surface states have 47%, 24%, and 13% of their density on the first three planes while the  $\bar{\Gamma}_4$  surface state has 80%, 16%, and 3.4%. Highly localized surface states and resonances like this at the center of the 2D BZ are essential, we believe, for explaining the observed<sup>7</sup> photoelectron spin-polarization reversal. The surface state is most localized at  $\bar{M}_2$  where its energy is  $-0.3721$  Ry,  $0.22$  Ry above the bulk continuum, and where over 99% of its density is on the surface plane. This is because the  $\bar{M}_2$  and  $\bar{M}_3$  states contain only  $x^2 - y^2$  basis functions on every other plane and the bulk  $\bar{M}_2$  and  $\bar{M}_3$  continua are only  $0.0001$  Ry wide. Because it lies above  $E_F$ , the  $\bar{M}_2$  surface state can

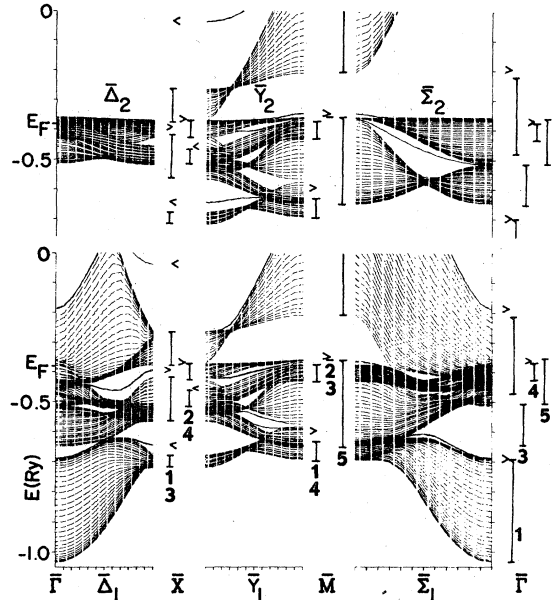


FIG. 4. Minority-spin subbands for 35-layer (100) Ni film.

cause it lies above  $E_F$ , the  $\bar{M}_2$  surface state can play no role in the photoemission. The  $\bar{\Gamma}_5$  surface state does not exist in the minority bands because the surface-parameter shift is not sufficiently large, however, a part of the surface-state band remains along  $\bar{\Delta}_2$ - $\bar{X}_2$ - $\bar{Y}_2$ - $\bar{M}_2$ - $\bar{\Sigma}_2$ . The  $\bar{\Gamma}_4$  surface state and its connecting resonance also remain.

In Figs. 5 and 6 we display the majority- and minority-spin subbands of the two symmetries along the symmetry lines of the rectangular 2D BZ for the 47-layer (110) film. Only a single surface state exists above the top of the majority-spin  $d$  bands at  $\bar{k}=0$ ; it has  $\bar{\Gamma}_2$  symmetry and is at  $-0.3941$  Ry, essentially the same energy as the (100)  $\bar{\Gamma}_5$  surface state. It is part of an  $\bar{X}_3$ - $\bar{\Sigma}_2$ - $\bar{\Gamma}_2$ - $\bar{\Delta}_2$ - $\bar{Y}_2$  surface-state band. It does not extend far enough along  $\bar{\Delta}$  to be present at the first  $\bar{\Delta}$  mesh point away from  $\bar{X}$ . However, a weak resonance exists along  $\bar{\Delta}$  somewhat below the top of the  $d$  bands. A second surface-state band exists right on the top of the  $d$  bands at  $\bar{Y}_2$  extending along  $\bar{\Delta}_2$  about  $\frac{5}{8}$  of the way to  $\bar{\Gamma}$ . As usual, a large number of surface-state bands can be seen in energy gaps throughout the 2D BZ.

#### IV. PHOTOELECTRON SPIN POLARIZATION

Earlier photoemission studies<sup>22</sup> as well as tunneling<sup>23</sup> experiments on nickel thin films indicated a net positive spin polarization for electrons just below the Fermi level. Recently Eib and Alvarado<sup>7</sup> found that the polarization of photoelectrons emitted from a (100) single-crystal nickel surface was negative at threshold but changed sign  $0.1$  eV above

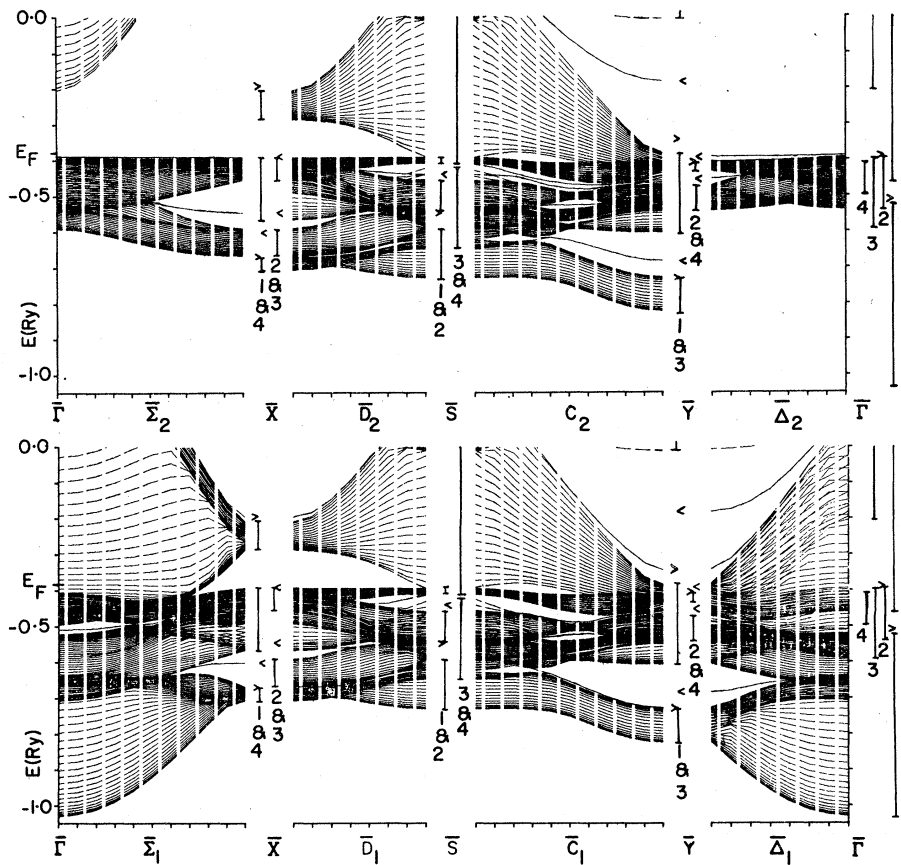


FIG. 5. Majority-spin sub-bands of  $\bar{\Sigma}_1-\bar{D}_1-\bar{C}_1-\bar{\Delta}_1$  and  $\bar{\Sigma}_2-\bar{D}_2-\bar{C}_2-\bar{\Delta}_2$  symmetry for 47-layer (110) Ni film.

threshold. This is believed to be consistent with the earlier results because of inhomogeneities in the work function of polycrystalline films. They claimed their measurements could not be explained by simple band theory. This was refuted by Wohlfarth<sup>24</sup> who pointed out that he had actually anticipated the experimentally observed polarization reversal.<sup>25</sup> However, Wohlfarth's calculation is based on a highly over simplified model DOS and neglects all consideration of wave-vector conservation. He assumes

$$J_{\sigma}(\omega) = \int_{-\hbar\omega}^{E_f} n_{\sigma}(E) dE, \quad (4)$$

where  $n_{\sigma}(E)$  is the bulk DOS of spin  $\sigma$ . We have generalized Eq. (4) to take the surface into account

$$J_{i\sigma}(\omega) = \int_{-\hbar\omega}^{E_f} n_{i\sigma}(E) dE, \quad (5)$$

where  $n_{i\sigma}(E)$  is given by Eqs. (2) and (3), and

$$J_{\sigma}(\omega) = \sum_{i=0} J_{i\sigma} e^{-i/l}. \quad (6)$$

Here the planes are numbered inward from the (zeroth) surface plane,  $l$  is the escape depth in interplanar spacings ( $l$  is between<sup>7</sup> 3 and 6) and

$$P = (J_{\uparrow} - J_{\downarrow}) / (J_{\uparrow} + J_{\downarrow}). \quad (7)$$

Before calculating  $P$  we rigidly raised the majority bands by 0.004 Ry (which raised  $E_F$  by 0.0004 Ry) and reduced the magneton number to 0.52. Any further rise of the majority bands would increase the discrepancy with the experimental value of 0.56 beyond what we believe the uncertainty in the experimental value to be. In Fig. 7 we display the polarization assuming only the surface plane ( $P_S$ ) or only the central plane ( $P_C$ ) contribute to the current (the latter corresponds to Wohlfarth's bulk DOS calculation) as well as the polarization with contributions from all planes with the escape depth  $l$  in Eq. (6) taken to be 4.5 interplanar spacings. Note that  $P_C$  stays close to  $-82\%$  until 0.14 eV above threshold where transitions from the top of the bulk-majority-spin  $d$  bands become possible and then rises, becoming positive at 0.42 eV above threshold but attains a maximum value of only 7%. Because the surface-state band just above the top of the majority-spin  $d$  bands crosses  $E_F$ ,  $P_S$  starts at  $-71\%$  and rises immediately (due to surface-state contributions to  $J_{\uparrow}$ ) becoming positive 0.12 eV above threshold. However, it never exceeds 15%. Because of the large value of  $l$  the polarization curve with contributions from all planes is



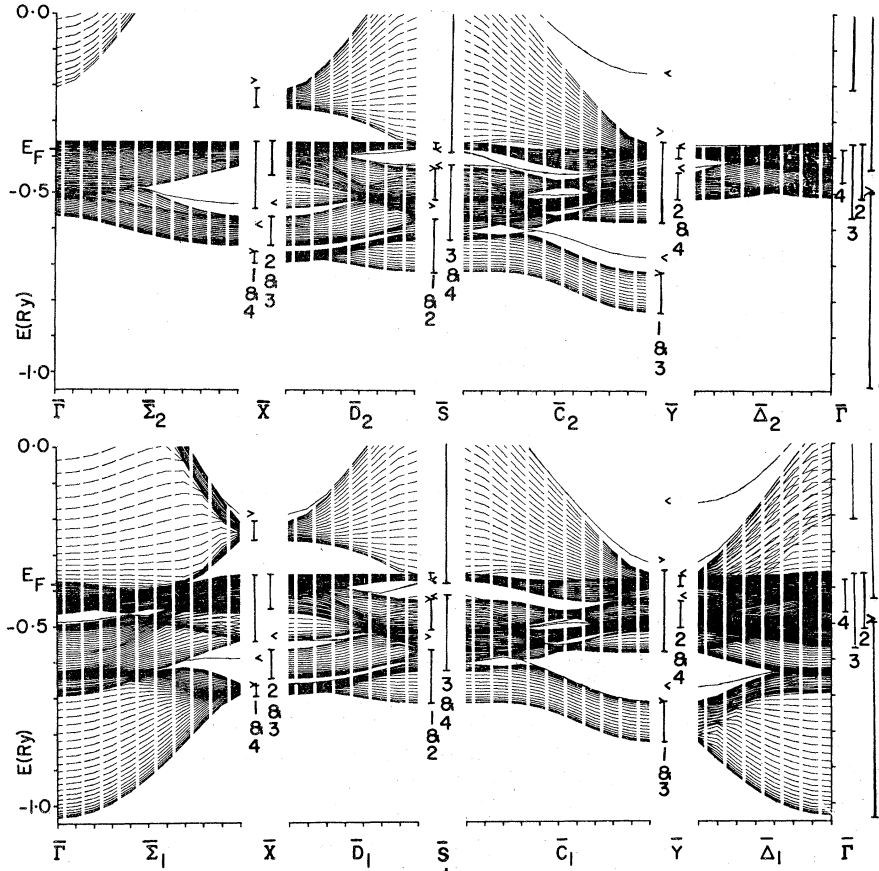


FIG. 6. Minority-spin sub-band for 47-layer (110) film.

very similar to  $P_c$  and quite unlike the experimental curve.<sup>7</sup>

Smith and Traum<sup>26</sup> pointed out that if wave vector  $\vec{k}$  is conserved in the optical excitation event, it is the joint DOS, not the DOS, which must be used in the calculation. They found the polarization jumped from  $-100\%$  to  $+100\%$  at 0.1 eV above threshold. They neglected conservation of  $\bar{k}$ , the transverse component of  $\vec{k}$ , upon escape. The three step (excitation, transport, and escape) process they consider actually contributes nothing to the photocurrent near threshold if  $\bar{k}$  is conserved, i.e., electrons which can be excited to positive energies for  $\hbar\omega$  close to threshold all have  $E < \bar{k}^2$  and cannot escape. This can easily be seen in Figs. 3 and 4 where there is a large gap in the region of  $E=0$ ,  $\bar{k}=0$ . We believe for an ideal surface the only allowed photoemission mechanism near threshold is a single-step excitation into an evanescent LEED state. This must also be true for real surfaces prepared sufficiently well for angle-resolved photoemission to be meaningful. Note that the three-step process, when allowed, may be considered to be a one-step process into a propagating (time-reversed) LEED state.<sup>27</sup> For our  $\bar{k}$ -conserving process  $n_{i\sigma}$  in Eq. (5) must be replaced by

$$D_{i\sigma}(E) = N^{-1} \sum_{j\alpha\beta n\vec{k}} W(\vec{k}) C_{\alpha i}^{n\vec{k}\sigma} S_{ij}^{\alpha\beta}(\sigma, \vec{k}) C_{\beta j}^{n\vec{k}\sigma} \times \delta(E - E_{n\vec{k}} + \bar{k}^2) \Theta(E_F - E_{n\vec{k}}), \quad (8)$$

where  $\Theta$  is a step function and other quantities are as in Eq. (2). In addition we must replace  $l^{-1}$  in Eq. (6) by twice the decay constant of the evanescent LEED state. This we approximate by  $\alpha = \sqrt{\delta E}$ , where  $\delta E$  is the distance to a propagating state. The gap at  $\bar{k}=0$  extends between  $-0.20$  and  $0.16$  Ry so we have  $2\alpha = 2\sqrt{0.16} = 0.8 \text{ bohr}^{-1} = 2.66 (\text{interplanar spacings})^{-1}$ . In Fig. 8 we display the polarization due to the central plane and due to the surface plane. Because of the large value of  $2\alpha$  the polarization as calculated from all planes is indistinguishable from the surface plane curve. Because only a single point in the 2D BZ ( $\bar{k}=0$ ) contributes within 0.04 eV of threshold (using our 576 point sample of the 2D BZ), we doubled the number of points sampled in the 2D BZ for  $\bar{k}^2 < 0.08$  Ry. Even so, because of the discreteness of the sample and because of the discreteness of the  $sp$  bands in a 35-layer film, we happen not to obtain any majority-spin  $sp$  contribution near threshold and the calculated  $P_{\text{threshold}} = -100\%$ . The Wohlfarth calculation which samples the entire 2D BZ yielded

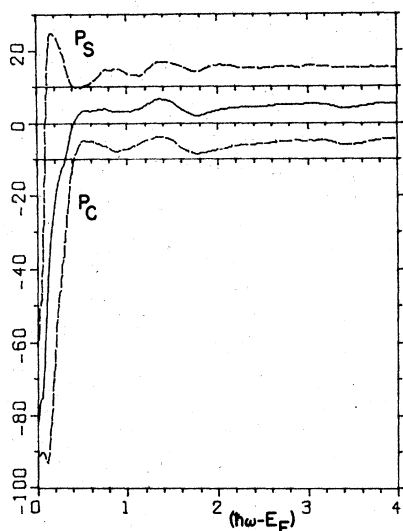


FIG. 7. The (100) Ni photoelectron spin polarization calculated according to the wave vector nonconserving Wohlfarth mechanism using the surface plane only ( $P_S$ ), the central plane only ( $P_C$ ), and from all planes with  $l = 4.5$  (solid curve). Note that the  $P_S$  and  $P_C$  curves are displaced by  $\pm 10\%$ .

$P_{\text{threshold}} = -82\%$  and that is probably a reasonable estimate for  $P_{\text{threshold}}$  with  $\bar{k}$  conservation.  $P$  starts rising rapidly 0.084 eV above threshold when the majority-spin  $\Gamma_5$  surface state start to contribute to the current, reverses sign 0.12 eV above threshold, continues rising aided by contributions from the majority-spin  $\Gamma_4$  surface state which commence 0.188 eV above threshold, and reaches a maximum value of 32% at 0.36 eV above threshold. This is to be compared with the experimental<sup>17</sup> maximum of 36%. The peak of our  $P$  curve is not so broad as the experimental curve. This is a consequence of using the threshold value of  $\alpha$  everywhere. As the energy increases, more LEED states with smaller  $\alpha$ 's become available until at about 2.1 eV above threshold transitions to propagating LEED states occur.<sup>28</sup> The  $P_C$  curve in Fig. 8, which barely becomes positive 3.4 eV above threshold, indicates that, even if we could raise the majority-spin bands relative to the minority still further without completely destroying agreement with the magneton number, we could not account for the photoelectron spin polarization of (100) Ni using bulk properties. Because there are propagating final states available at threshold, we have not repeated this calculation for (110) Ni. However, because of the competition with transitions to these propagating states and because there exists only a single surface state above the top of the majority  $d$  bands,

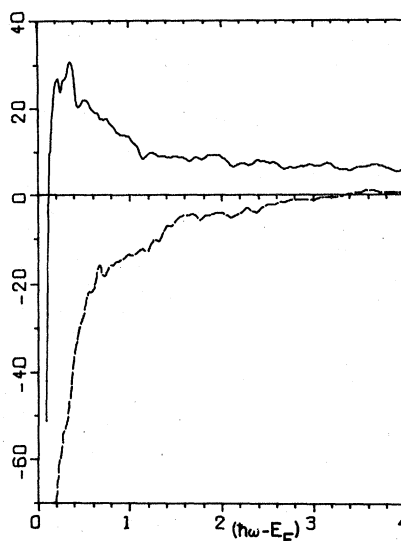


FIG. 8. The (100) Ni photoelectron spin polarization calculated for  $\bar{k}$ -conserving transitions into evanescent LEED states using the central plane  $D_{i\sigma}$  (dashed curve) and surface plane  $D_{i\sigma}$  (solid curve). The polarization calculated from all planes is indistinguishable from the solid curve.

we would predict that the photoelectron spin polarization from the (110) face of Ni does not change as rapidly as it does for the (100) face.

There have been proposed<sup>29, 30</sup> many-electron explanations of the spin-polarization reversal based on the single-band Hubbard Hamiltonian. We have<sup>31</sup> recently argued that the single-band Hubbard Hamiltonian is a completely inappropriate model for Ni and estimated the many-body contributions to the self-energy to be less than 0.01 eV. There are two important points to be made. The first is that, even if many-body effects should turn out to be important, because of the lack of propagating final states at threshold, those many-body effects must be calculated at the surface. The second is that in order to have the extremely rapid rise in the polarization curve there must be extremely sharp structure in the DOS (more exactly, in the one-dimensional DOS at  $\bar{k} = 0$ ) such as that caused by surface states. It is hard to see how large many-body effects could fail to contain a large imaginary self-energy contribution which would wipe out that structure.

#### ACKNOWLEDGMENTS

This work was supported by the NSF under Grant Nos. DMR 73-02449-A02 and DMR 77-21559, 21559.

- <sup>1</sup>J. G. Gay, J. R. Smith, and F. J. Arlinghaus, *Phys. Rev. Lett.* **38**, 561 (1977).
- <sup>2</sup>E. Caruthers, D. G. Dempsey, and L. Kleinman, *Phys. Rev. B* **14**, 288 (1976).
- <sup>3</sup>R. V. Kasowski, *Phys. Rev. B* **14**, 3398 (1976), and references therein.
- <sup>4</sup>D. G. Dempsey, L. Kleinman and E. Caruthers, (a) *Phys. Rev. B* **12**, 2932 (1975); (b) **13**, 1489 (1976); (c) **14**, 279 (1976).
- <sup>5</sup>K. S. Sohn, D. G. Dempsey, L. Kleinman and E. Caruthers, (a) *Phys. Rev. B* **13**, 1515 (1976); (b) **14**, 3193 (1976); (c) **14**, 3185 (1976).
- <sup>6</sup>O. Bisi, C. Calandra, and F. Manghi, *Solid State Commun.* **23**, 249 (1977); C. M. Bertoni, C. Calandra, and F. Manghi, *ibid.* **23**, 255 (1977).
- <sup>7</sup>W. Eib and S. F. Alvarado, *Phys. Rev. Lett.* **37**, 444 (1976).
- <sup>8</sup>G. P. Alldredge and L. Kleinman, *Phys. Rev. B* **10**, 559 (1974).
- <sup>9</sup>D. G. Dempsey and L. Kleinman, *J. Phys. F* **7**, 113 (1977).
- <sup>10</sup>D. G. Dempsey and L. Kleinman, *Phys. Rev. B* **16**, 5356 (1977).
- <sup>11</sup>K. S. Sohn, D. G. Dempsey, L. Kleinman, and G. P. Alldredge, *Phys. Rev. B* **16**, 5367 (1977).
- <sup>12</sup>C. S. Wang and J. Callaway, *Phys. Rev. B* **15**, 298 (1977). Hereafter called WC.
- <sup>13</sup>P. W. Anderson, *Phys. Rev.* **181**, 25 (1969).
- <sup>14</sup>D. G. Dempsey and L. Kleinman (unpublished).
- <sup>15</sup>M. Mehta and C. S. Fadley, *Phys. Rev. Lett.* **39**, 1569 (1977).
- <sup>16</sup>J. C. Slater and G. F. Koster, *Phys. Rev.* **94**, 1498 (1954).
- <sup>17</sup>J. E. Demuth, P. M. Marcus, and D. W. Jepsen, *Phys. Rev. B* **11**, 1460 (1975).
- <sup>18</sup>C. M. Chan, S. L. Cunningham, M. A. van Hove, and W. H. Weinberg, *Surf. Sci.* **67**, 1 (1977).
- <sup>19</sup>D. G. Dempsey and L. Kleinman, *Phys. Rev. Lett.* **39**, 1298 (1977).
- <sup>20</sup>There are 9 basis functions per plane times 47 planes times 88 independent  $\bar{k}$  [= 37,224 for the (110) film]. For the (100) film the numbers are 9 times 35 times 91 = 28 665 from which a number of order 70 must be subtracted because of degeneracies at the center and corner of the square  $2D$  BZ.
- <sup>21</sup>For a listing of the basis functions in eigenfunctions of different symmetries see Ref. 4(a) for (100) films and Ref. 5(b) for (110).
- <sup>22</sup>U. Banninger, G. Busch, M. Campagna, and H. C. Siegmann, *Phys. Rev. Lett.* **25**, 585 (1970).
- <sup>23</sup>P. M. Tedrow and R. Meservey, *Phys. Rev. Lett.* **26**, 192 (1971).
- <sup>24</sup>E. P. Wohlfarth, *Phys. Rev. Lett.* **38**, 524 (1977).
- <sup>25</sup>E. P. Wohlfarth, *Phys. Lett. A* **36**, 131 (1971).
- <sup>26</sup>N. V. Smith and M. M. Traum, *Phys. Rev. Lett.* **27**, 1388 (1971).
- <sup>27</sup>D. J. Spanjaard, D. W. Jepsen, and P. M. Marcus, *Phys. Rev. B* **15**, 1728 (1977).
- <sup>28</sup>Reference 19 erroneously states this occurs 1 eV above threshold.
- <sup>29</sup>P. W. Anderson, *Philos. Mag.* **24**, 203 (1971).
- <sup>30</sup>J. A. Hertz and D. M. Edwards, *J. Phys. F* **3**, 2174 and 2191 (1973).
- <sup>31</sup>L. Kleinman, *Phys. Rev. B* **17**, 3666 (1978).